NANO LETTERS

Letter

pubs.acs.org/NanoLett

Bacterial Recognition of Silicon Nanowire Arrays

Hoon Eui Jeong,[†,‡] Ilsoo Kim,[§] Pierre Karam,[†] Heon-Jin Choi,[§] and Peidong Yang*[,†]

[†]Department of Chemistry, University of California, Berkeley, California 94720, United States

[‡]School of Mechanical and Advanced Materials Engineering, Ulsan National Institute of Science and Technology, Ulsan 689-798, South Korea

[§]Department of Materials Science and Engineering, Yonsei University, Seoul 120-749, South Korea

Supporting Information

ABSTRACT: Understanding how living cells interact with nanostructures is integral to a better understanding of the fundamental principles of biology and the development of next-generation biomedical/bioenergy devices. Recent studies have demonstrated that mammalian cells can recognize nanoscale topographies and respond to these structures. From this perspective, there is a growing recognition that nanostructures, along with their specific physicochemical properties, can also be used to regulate the responses and motions of bacterial cells. Here, by utilizing a well-defined silicon nanowire array platform and single-cell imaging, we present direct evidence that *Shewanella oneidensis* MR-1 can recognize nanoscale structures and that their swimming patterns and initial attachment locations are strongly influenced by the presence of nanowires on a surface. Analyses of bacterial trajectories revealed that MR-1 cells exhibited a confined diffusion mode in the presence of nanowires and showed preferential attachment to the nanowires, whereas a superdiffusion mode was observed in the absence of nanowires. These results demonstrate that nanoscale topography can affect bacterial movement and attachment and play an important role during the early stages of biofilm formation.

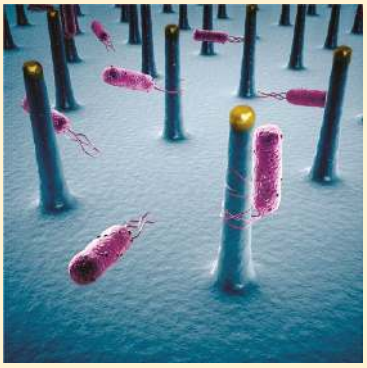

KEYWORDS: *Nanowires, bacteria, diffusion, single-cell imaging, trajectory analysis*

Nanoengineered surfaces that can regulate bacterial attachment are potentially useful for developing microbial fuel cells with high power densities and antibacterial biomedical devices.[1−5] Nanostructured electrodes have been developed to enhance the power density of microbial fuel cells by promoting bacterial attachment to the electrode surface.[1,2] Nanostructured materials have also been explored as antibacterial surfaces that are resistant to biofilm formation.[3−5] While much effort has been expended on the development of nanoengineered surfaces that can control bacterial motion and attachment on surfaces, the fundamental principles of bacteria−nanostructure interactions remain poorly understood. Different bacterial behaviors on nanostructured substrates have been reported. Some studies reported that nanostructures had no significant effects on bacterial attachment, whereas others reported that nanoscale topographies did influence the attachment and growth of bacteria.[4−9] Moreover, most previous works were based on observations of large bacterial populations cultured on a surface with random nanostructures.[5−9] While these approaches are useful for studying bacterial film formation at the macroscopic level, randomly oriented, high-density nanostructures and massive bacterial populations make it difficult to investigate bacteria−nanostructure interactions in a systematic manner.[4−9]

In this respect, nanowires can be a powerful platform for studying bacteria−nanostructure interactions at the single-cell level. Recent studies have shown that nanowires can interface with mammalian cells in a minimally invasive manner because of their nanoscale dimensions.[10−13] In addition to mammalian cells, nanowires are also promising for interfacing with bacterial cells, since their nanoscale dimensions (100−300 nm) are comparable to those of individual bacterial cells. Interfacing nanowires with single bacterial cells will enable us to investigate in detail how individual bacteria interact with surfaces. In addition, nanowires can be produced in precisely ordered arrays with accurate size and position control, allowing systematic study of bacteria−nanostructure interactions for nanowires with different geometries.[14] Furthermore, the unique electrical properties of nanowires and surface functionalizations of nanowires would potentially allow electrical and chemical stimuli to be applied through the nanowires.[12]

Here, by combining a precisely defined silicon nanowire array platform and real-time optical imaging, we explore bacteria−nanostructure interactions at the single-cell level. In this study, *Shewanella oneidensis* MR-1, a gram-negative facultative bacterium, was used as a model microorganism to study bacteria−nanostructure interactions, since *S. oneidensis* MR-1 is well-known for its biofilm formation on mineral surfaces and electrodes of microbial fuel cells.[15−17] The trajectories of MR-1 cells on substrates with Si nanowire arrays

Received: April 4, 2013
Revised: May 8, 2013
Published: May 17, 2013

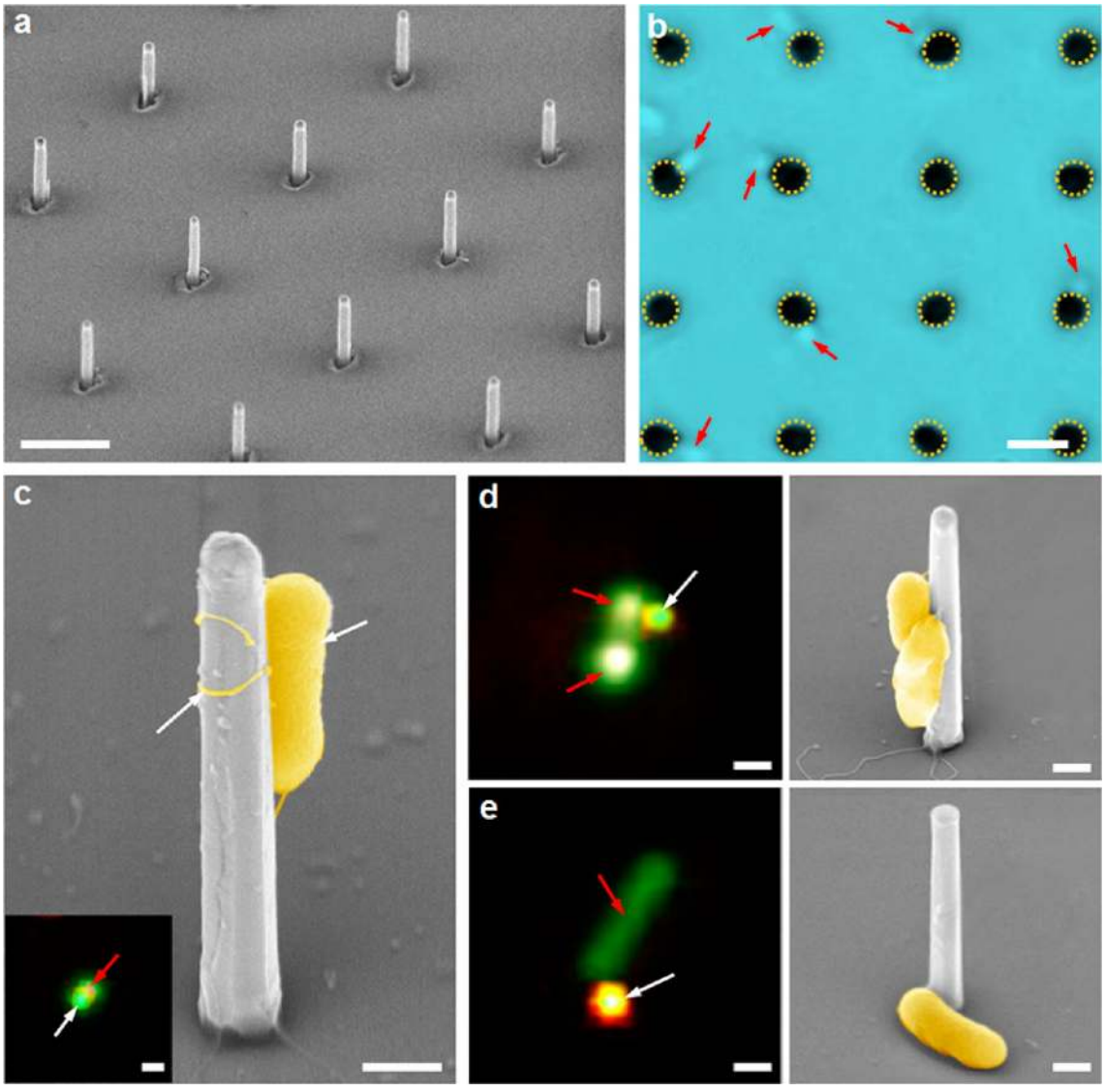

Figure 1. *Shewanella oneidensis* MR-1 grown on patterned Si nanowire arrays. (a) Titled SEM image of the patterned Si nanowire arrays on a Si(111) substrate. The pitch of the arrays is 10 μm and the diameter and length of the individual nanowires are ~300 nm and ~3 μm, respectively. (b) Bright-field micrograph of *Shewanella oneidensis* MR-1 grown on the Si nanowire arrays. Scale bars in panels a and b, 5 μm. (c–e) SEM images showing MR-1 cells attached on the Si nanowires and their corresponding merged images of fluorescence micrographs of stained MR-1 and dark-field micrographs of Si nanowires. Single (c) or multiple (d) MR-1 cells were preferentially attached on the individual nanowires with alignments along the length direction of the nanowires. Some cells were observed on the bottom substrate, but many of them still maintained close contact with the nanowires (e). Scale bars in panels c–e, 500 nm.

were analyzed and quantified by mathematical models. We show that MR-1 cells can recognize nanowires and that their swimming and attachment behaviors are drastically altered by the presence of nanowires on a substrate. Our novel approach based on interfacing between a nanowire and a single bacterial cell offers a new set of tools for systematically studying bacteria–surface interactions at the single-cell level.

Figure 1a shows the patterned Si nanowire arrays with a 10 μm pitch. The diameter and length of the individual nanowires are ~300 nm and ~3 μm, respectively. *Shewanella oneidensis* MR-1 was cultured on the Si nanowire arrays under aerobic or anaerobic conditions, and its motion was observed using upright microscopy. Interestingly, the majority of MR-1 cells attached directly to the Si nanowires (Figure 1b) rather than the bottom substrate. The scanning electron microscopy (SEM) images and their corresponding merged optical images (fluorescence and dark field) (Figure 1c–e) clearly indicate that the MR-1 bacterium attached preferentially to the Si nanowires. More interestingly, single MR-1 cells attached to individual Si nanowires in perfect alignment with the Si nanowires (Figure 1c). Occasionally, MR-1 cells were also observed sitting on the bottom substrate (Figure 1b, e).

When compared with prior approaches using substrates with random nanostructures,[5–9] our approach using patterned Si nanowire arrays allows accurate analyses of bacteria–nanostructure interactions to be performed at the single-cell level. Moreover, the surfaces of the Si nanowires can be easily functionalized with different chemicals. The size of the nanowires, including the diameter as well as the length, can be readily controlled by modulating the growth conditions.[14] Interestingly, when the size of a nanowire was comparable to that of an individual MR-1 bacterium and the bacterial density was low, we could readily induce a single MR-1 cell to attach to an individual Si nanowire. To examine the bacteria–nanowire

dx.doi.org/10.1021/nl401205b | *Nano Lett.* 2013, 13, 2864–2869

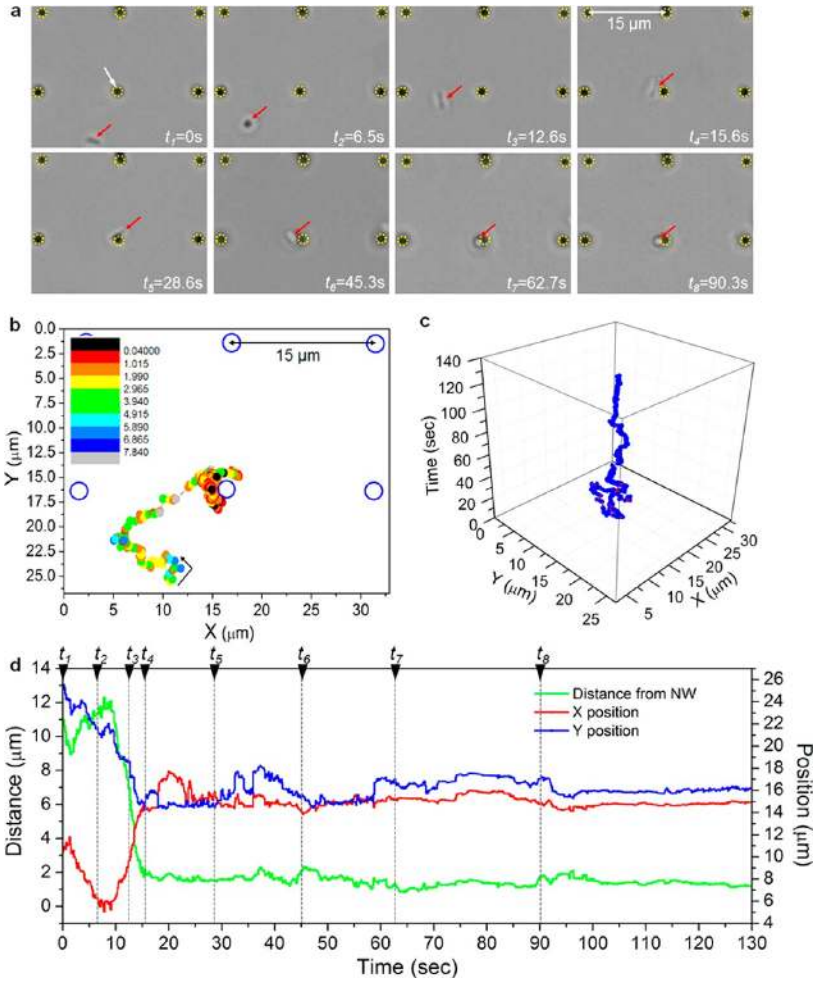

Figure 2. MR-1 bacterial motion and trajectory on Si nanowire arrays with a 15 μm pitch. (a) Time-lapse optical images of a single MR-1 bacterium on the array and (b) corresponding trajectory. (c,d) *X*, *Y* displacements of the MR-1 cell versus time. The 3D (c) and 2D (d) trajectory plots show confined movements around one specific Si nanowire after the bacterium encounters the nanowire at ~15 s.

interactions at the single-cell level, we made the dimension of the Si nanowires (~300 nm in diameter and ~3 μm in length) similar to that of an MR-1 bacterium (400−700 nm in width and 2−3 μm in length).

To confirm the observation of preferential attachment of MR-1 cells to Si nanowires, we performed real-time optical imaging of the MR-1 movements on the nanowire arrays. Nanowire arrays with relatively long pitches (10 and 15 μm) were used in these experiments. Figure 2a shows time-lapse images of the movements of a single MR-1 cell on an array with a 15 μm pitch. At the initial stage of the observation (Figure 2a), the MR-1 cell swam freely without binding to or sitting on the substrate. However, after the MR-1 cell encountered one of the nanowires at ~15 s, the cell stayed on the nanowire for a long period of time (>5 min) while changing the orientation of its body (see Supporting Information Figure S1 and Movie S1). To further investigate bacteria−nanowire interactions, we analyzed the trace of the bacterial movements using particle-tracking software. The analyzed trajectory (Figure 2b) clearly showed that the MR-1 bacterium stayed around the nanowire and had a diminished velocity after it approached the nanowire. Additional *X*, *Y* displacement analysis with time (Figure 2c,d) further confirmed that the MR-1 bacterium strongly preferred to stay on the Si nanowires rather than travel to the planar bottom Si substrate, although they both have the same Si/SiO_2 surface. As shown in Figure 2c,d, the position of the cell was almost fixed to the specific coordinate values where the Si nanowire was located after the cell encountered the nanowire at ~15 s, suggesting there is a distinct interaction between the MR-1 bacterium and the Si nanowire.

To investigate the effects of the pitch of the nanowire arrays on bacterial motions, we repeated the same optical imaging experiments on Si nanowire arrays with a 10 μm pitch (Figure 3a). Again, the trajectory of the bacterial movement was highly correlated with the nanowire locations (Figure 3a, b). Over the span of ~20 s, the MR-1 cell swam around four individual nanowires (Figure 3a and Supporting Information Movie S2), and its trajectory notably showed circular patterns around the nanowires (Figure 3b). According to previous studies, singly flagellated monotrichous bacteria exhibit a straight trajectory during forward motion whereas the trajectory tends to be circular during backward motion, especially when the cell swims close to a wall.[18,19] Interestingly, the MR-1 bacterial trajectory on the nanowire array in Figure 3 and Supporting Information Movie S2 also shows circular motion in a counterclockwise direction around the individual nanowires. This suggests that the MR-1 cell, which is also a singly flagellated monotrichous bacterium, swam backward while traveling around the nanowires. When the trajectory is dissected along its *X* and *Y* components and plotted versus time (Figure 3c), it can be

dx.doi.org/10.1021/nl401205b | *Nano Lett.* 2013, 13, 2864−2869

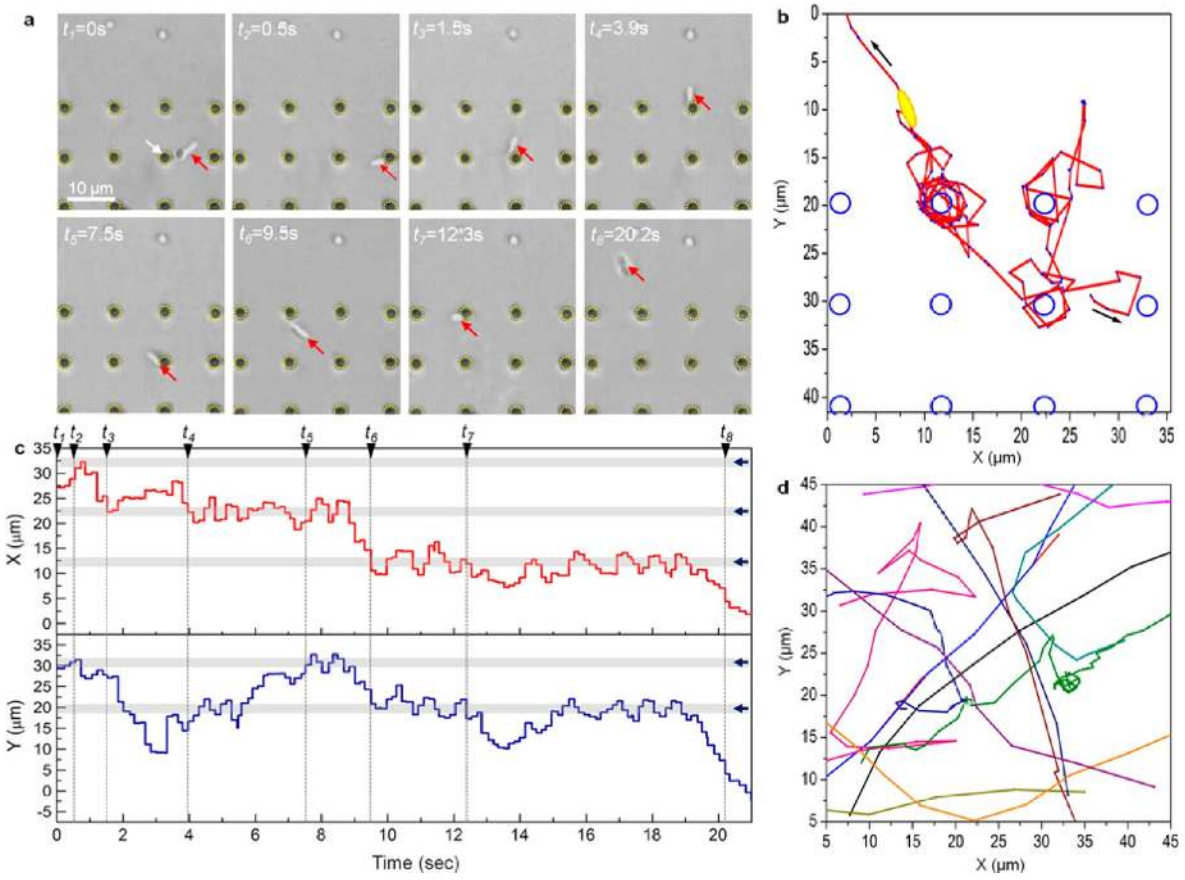

Figure 3. MR-1 bacterial motion and trajectory on Si nanowire arrays with a 10 μm pitch. (a) Time-lapse optical images of a single MR-1 bacterium on the array. The analyzed trajectory (b) shows confined bacterial motions around the Si nanowires. (c) *X*, *Y* displacements of the MR-1 cell versus time. Gray lines and navy arrows indicate positions where individual Si nanowires are located. (d) Trajectories of multiple MR-1 cells on a planar Si substrate showing random swimming patterns.

further confirmed that the cell dwelled on each nanowire for about 2−8 s before it went through a quick transition state (<1 s) and then stayed around another nanowire. No bacterial confinement was observed in the absence of nanowires. As shown in Figure 3d, the swimming traces of the MR-1 cells on a planar surface exhibited random-walk patterns. A direct comparison between Figure 3 panels b and d also shows that the swimming and attachment behaviors of the MR-1 bacteria are influenced significantly by the presence of nanoscale topography on a surface.

Additional optical imaging experiments were also performed to investigate the detailed process of how individual MR-1 cells attached to the Si nanowires over a longer observation time (Supporting Information Figure S2). During the observation, the MR-1 cells preferentially attached to the nanowires, but some of the attached MR-1 cells left the nanowires after just a few seconds or a few tens of seconds. This means that the bacterial attachment is reversible at this stage, which is a characteristic of the early stages of biofilm formations.[20,21] However, the number of cells attached to the nanowire arrays gradually increased with time (Supporting Information Figure S2). Interestingly, when we increased the length of the Si nanowires from 3 to 15−20 μm, multiple cells were observed to selectively sit on a single Si nanowire (Supporting Information Figure S2b). This initial but reversible MR-1 attachment to the Si nanowires observed here corresponds to the first step of bacterial biofilm formation. At this stage, bacteria use a variety of extracellular appendages and proteins for sensing and attaching to solid surfaces, including flagella, pili, fimbriae, curlifibers, and outer membrane proteins.[5,21−23] To investigate the relevant biological mechanisms, mutants of MR-1 bacteria lacking outer membrane cytochromes OmcA and MtrC, which are in charge of electron transfer across the cell membranes,[24] were cultured on the nanowire arrays. However, the MR-1 mutants still exhibited preferential movement toward and attachment to the Si nanowires. Experiments with flagella mutants have been excluded in our study because mutants of MR-1 bacteria lacking flagella are not able to swim and most of cells settle on the bottom substrate.[25,26] However, the SEM image shown in Figure 1c in which the MR-1 bacterium attached to the Si nanowire wraps the nanowire with its flagella may suggest the possibility that the bacteria sense the nanoscale structures by utilizing their cellular appendages as suggested in other studies.[22,23] Interestingly, the Si nanowire-confined swimming behaviors were also observed for other strains of bacteria such as *Escherichia coli* K-12 strains W3110 and MG1655 in separate experiments (data not shown). This suggests that the ability to sense nanoscale topographies is general for many bacterial strains that have evolved mechanisms for attaching to surfaces and forming biofilms for survival in diverse environmental conditions.[5,16,20−23] More studies are required to reveal the detailed biological mechanisms of the bacteria−nanostructure recognitions.

To quantify how the MR-1 bacteria are confined around nanowires, a set of swimming trajectories on planar Si substrates and substrates with nanowire arrays of 10 and 15

dx.doi.org/10.1021/nl401205b | *Nano Lett.* 2013, 13, 2864−2869

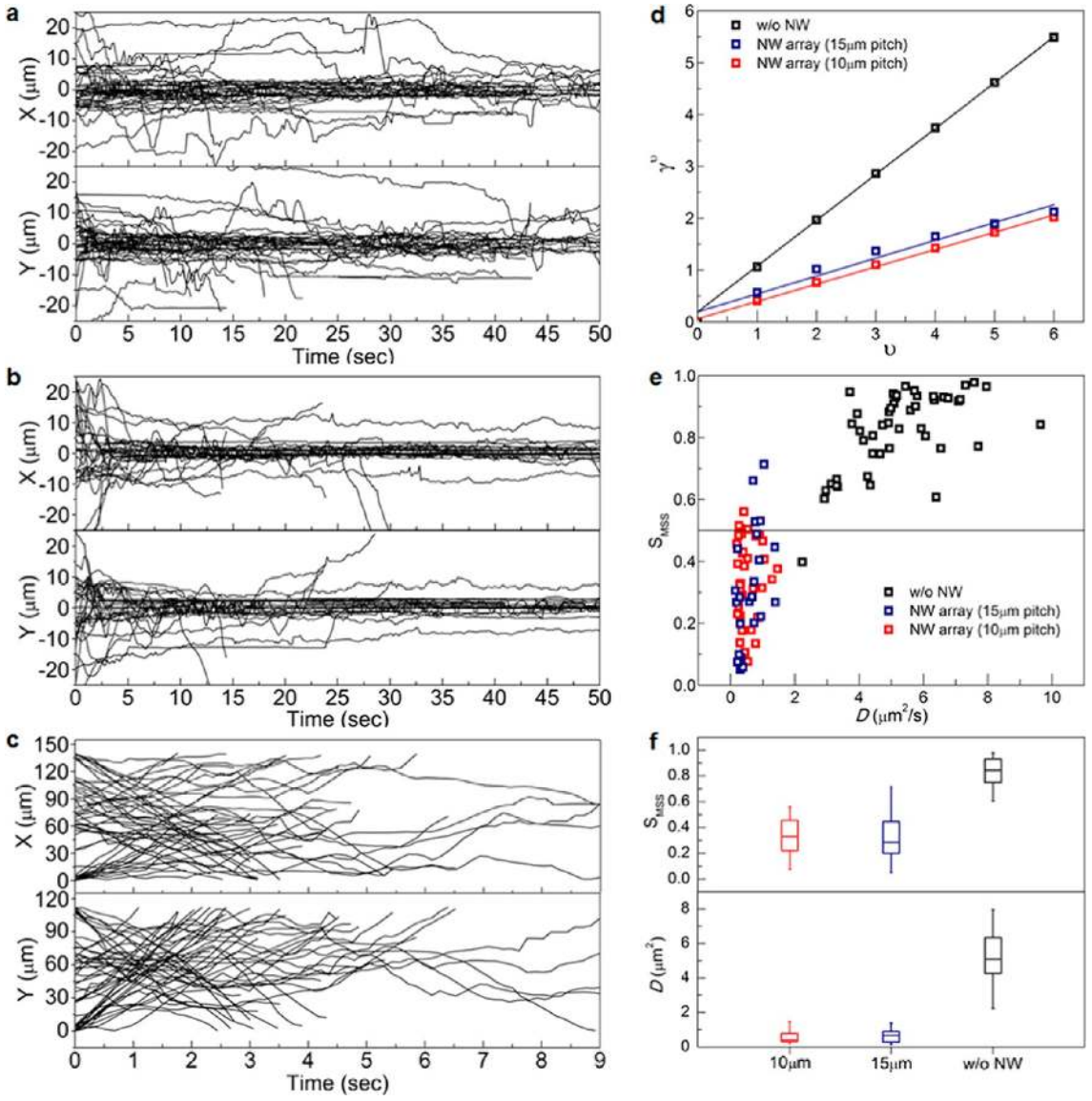

Figure 4. Quantitative analysis of MR-1 bacterial motions on different substrates. (a–c) *X*, *Y* displacements of multiple MR-1 cells versus time on each substrate with Si nanowire arrays with a pitch of 10 μm (a) and 15 μm (b), and without Si nanowires (c). (d) Moment scaling spectra (MSS) of the representative bacterial trajectories on each substrate. Among multiple bacterial trajectories on each substrate, trajectories having S_{MSS} close to the average S_{MSS} for each substrate were selected and plotted here as representatives for each substrate. (e) S_{MSS}/D scatter plot of MR-1 trajectories on a planar Si substrate (black) and substrates with 15 μm pitch (blue) and 10 μm pitch (red) nanowire arrays. (f) Averages of S_{MSS} and D from multiple trajectories on each substrate shown in (e).

μm pitches were collected from multiple imaging experiments, and the *X* and *Y* displacements were plotted versus time (Figure 4a–c). As shown in Figure 4a,b, in the presence of nanowires the positions of the MR-1 cells were mostly confined to the specific *X* and *Y* coordinate values (0, ±10, and ±20 μm for the array with a 10 μm pitch and 0 and ±15 μm for the array with a 15 μm pitch) where individual Si nanowires were located. On the other hand, the trajectories of the bacteria were completely scattered over time in the absence of nanowires (Figure 4c). These differences were classified and quantified using the moment scaling spectrum (MSS) theory.[27,28] This method enables the classification and quantification of dispersive particle motions. The analysis of particle motion is based on calculating the moments of the displacements of individual particles.[27,28] Assuming that each moment $\mu_\nu(\delta t)$ depends on the time shift (δt) according to a power law $\mu_\nu(\delta t) \propto \delta t^{\gamma\nu}$, all scaling coefficients γ^ν for each moment order ν are determined by a linear least-squares regression to log $\mu_\nu(\delta t)$ versus log(δt). In addition, the two-dimensional diffusion coefficients can be calculated from the *y*-axis intercepts y_0. The plot of γ^ν (scaling coefficient) versus ν (moment order) is termed the MSS, and the slope of the MSS (S_{MSS}) is a reliable criterion for distinguishing different modes of motion. An S_{MSS} value between 0 and 0.5 indicates subdiffusion (e.g., confined diffusion), and a value between 0.5 and 1 represents superdiffusion (e.g., diffusion with a deterministic drift).[27,28] By plotting γ^ν versus ν (Figure 4d) and S_{MSS} versus diffusion coefficient (D) (Figure 4e), we could distinguish and classify the modes of bacterial motion on the substrates with and without nanowires. As shown in Figure 4d–f, noticeable differences in the modes of bacterial motion were found in the presence and absence of nanowires. In the absence of

dx.doi.org/10.1021/nl401205b | *Nano Lett.* 2013, 13, 2864–2869

nanowires, the MR-1 cells were observed to have a super-diffusion mode of motion with an S_{MSS} of 0.821 ± 0.130 and a diffusion coefficient (D) of 5.279 ± 1.538 $\mu m^2/s$ (n = 92). However, in the presence of nanowires, significant drops in the slope of the MSS and the diffusion coefficient were observed (Figure 4d–f). Most of the analyzed trajectories exhibited the characteristics of a confined diffusion mode. For the 10 and 15 μm pitch array, the S_{MSS} was 0.334 ± 0.138 and 0.314 ± 0.188, respectively and the diffusion coefficient was 0.546 ± 0.323 $\mu m^2/s$ (n = 36) and 0.616 ± 0.370 $\mu m^2/s$ (n = 28), respectively. The decreases in the diffusion constant and S_{MSS} are mainly due to the dwelling times that each MR-1 cell spent in the vicinity of the nanowires.

Our results demonstrate that nanoscale topographies on surfaces play an important role during the early stage of biofilm formation. Understanding the origins of biofilm formation at the single-cell level could provide a wealth of information for advancing the fundamentals of microbiology and designing next-generation bioenergy and biomedical devices. Our current approach based on precisely defined nanowire arrays and real-time single-cell imaging can serve as a powerful platform for studying bacteria–surface interactions under varying chemical, physical, electrical, and optical conditions at the single-cell level.

■ ASSOCIATED CONTENT

Supporting Information

Additional information and figures. This material is available free of charge via the Internet at http://pubs.acs.org.

■ AUTHOR INFORMATION

Corresponding Author

*E-mail: p_yang@berkeley.edu.

Notes

The authors declare no competing financial interest.

■ ACKNOWLEDGMENTS

P.Y. Thanks the National Science Foundation for the A. T. Waterman award. The authors thank the CISMM at UNC–CH for video spot tracking software, and Y. J. Hwang for discussion. H.J.C. and I.K. thank the National Research Foundation of Korea for the grant (No. 2012R1A2A1A03010558) and the Pioneer Research Program for Converging Technology (No. 2009-008-1529).

■ REFERENCES

(1) Xie, X.; Hu, L. B.; Pasta, M.; Wells, G. F.; Kong, D. S.; Criddle, C. S.; Cui, Y. *Nano Lett.* **2011**, *11*, 291–296.
(2) Mink, J. E.; Rojas, J. P.; Logan, B. E.; Hussain, M. M. *Nano Lett.* **2012**, *12*, 791–795.
(3) Mitik-Dineva, N.; Wang, J.; Truong, V. K.; Stoddart, P.; Malherbe, F.; Crawford, R. J.; Ivanova, E. P. *Curr. Microbiol.* **2009**, *58*, 268–273.
(4) Hochbaum, A. I.; Aizenberg, J. *Nano Lett.* **2010**, *10*, 3717–3721.
(5) Renner, L. D.; Weibel, D. B. *MRS Bull.* **2011**, *36*, 347–355.
(6) Puckett, S. D.; Taylor, E.; Raimondo, T.; Webster, T. J. *Biomaterials* **2010**, *31*, 706–713.
(7) Jeyachandran, Y. L.; Venkatachalam, S.; Karunagaran, B.; Narayandass, S. K.; Mangalaraj, D.; Bao, C. Y.; Zhang, C. L. *Mater. Sci. Eng., C* **2007**, *27*, 35–41.
(8) Rizzello, L.; Sorce, B.; Sabella, S.; Vecchio, G.; Galeone, A.; Brunetti, V.; Cingolani, R.; Pompa, P. P. *ACS Nano* **2011**, *5*, 1865–1876.
(9) Akesso, L.; Pettitt, M.; Callow, J.; Callow, M.; Stallard, J.; Teer, D.; Liu, C.; Wang, S.; Zhao, Q.; D'Souza, F.; Willemsen, P.; Donnelly, G.; Donik, C.; Kocijan, A.; Jenko, M.; Jones, L.; Guinaldo, P. C. *Biofouling* **2009**, *25*, 55–67.
(10) Yan, R.; Park, J.-H.; Choi, Y.; Heo, C.-J.; Yang, S.-M.; Lee, L. P.; Yang, P. *Nat. Nanotechnol.* **2012**, *7*, 191–196.
(11) Kim, W.; Ng, J. K.; Kunitake, M. E.; Conklin, B. R.; Yang, P. *J. Am. Chem. Soc.* **2007**, *129*, 7228–7729.
(12) Yang, P. D.; Yan, R. X.; Fardy, M. *Nano Lett.* **2010**, *10*, 1529–1536.
(13) Shalek, A. K.; Robinson, J. T.; Karp, E. S.; Lee, J. S.; Ahn, D. R.; Yoon, M. H.; Sutton, A.; Jorgolli, M.; Gertner, R. S.; Gujral, T. S.; MacBeath, G.; Yang, E. G.; Park, H. *Proc. Natl. Acad. Sci. U.S.A.* **2010**, *107*, 1870–1875.
(14) Hochbaum, A. I.; Fan, R.; He, R.; Yang, P. *Nano Lett.* **2005**, *5*, 457–460.
(15) Gorby, Y. A.; Yanina, S.; McLean, J. S.; Rosso, K. M.; Moyles, D.; Dohnalkova, A.; Beveridge, T. J.; Chang, I. S.; Kim, B. H.; Kim, K. S.; Culley, D. E.; Reed, S. B.; Romine, M. F.; Saffarini, D. A.; Hill, E. A.; Shi, L.; Elias, D. A.; Kennedy, D. W.; Pinchuk, G.; Watanabe, K.; Ishii, S.; Logan, B.; Nealson, K. H.; Fredrickson, J. K. *Proc. Natl. Acad. Sci. U.S.A.* **2006**, *103*, 11358–11363.
(16) Lower, S. K.; Hochella, M. F.; Beveridge, T. J. *Science* **2001**, *292*, 1360–1363.
(17) Lovley, D. R. *Nat. Rev. Microbiol.* **2006**, *4*, 497–508.
(18) Goto, T.; Nakata, K.; Baba, K.; Nishimura, M.; Magariyama, Y. *Biophys. J.* **2005**, *89*, 3771–3779.
(19) Taylor, B. L.; Koshland, D. E. *J. Bacteriol.* **1974**, *119*, 640–642.
(20) Kolter, R.; Greenberg, E. P. *Nature* **2006**, *441*, 300–302.
(21) McDougald, D.; Rice, S. A.; Barraud, N.; Steinberg, P. D.; Kjelleberg, S. *Nat. Rev. Microbiol.* **2012**, *10*, 39–50.
(22) Thormann, K. M.; Saville, R. M.; Shukla, S.; Pelletier, D. A.; Spormann, A. M. *J. Bacteriol.* **2004**, *186*, 8096–8104.
(23) Pratt, L. A.; Kolter, R. *Mol. Microbiol.* **1998**, *30*, 285–293.
(24) Xiong, Y. J.; Shi, L.; Chen, B. W.; Mayer, M. U.; Lower, B. H.; Londer, Y.; Bose, S.; Hochella, M. F.; Fredrickson, J. K.; Squier, T. C. *J. Am. Chem. Soc.* **2006**, *128*, 13978–13979.
(25) Bouhenni, R. A.; Vora, G. J.; Biffinger, J. C.; Shirodkar, S.; Brockman, K.; Ray, R.; Wu, P.; Johnson, B. J.; Biddle, E. M.; Marshall, M. J.; Fitzgerald, L. A.; Little, B. J.; Fredrickson, J. K.; Beliaev, A. S.; Ringeisen, B. R.; Saffarini, D. A. *Electroanalysis* **2010**, *22*, 856–864.
(26) Friedlander, R. S.; Vlamakis, H.; Kim, P.; Khan, M.; Kolter, R.; Aizenberg, J. *Proc. Natl. Acad. Sci. U.S.A.* **2013**, *110*, 5624–5629.
(27) Ferrari, R.; Manfroi, A. J.; Young, W. R. *Phys. D* **2001**, *154*, 111–137.
(28) Ewers, H.; Smith, A. E.; Sbalzarini, I. F.; Lilie, H.; Koumoutsakos, P.; Helenius, A. *Proc. Natl. Acad. Sci. U.S.A.* **2005**, *102*, 15110–15115.

■ NOTE ADDED AFTER ASAP PUBLICATION

The Acknowledgments have been updated. The revised version was re-posted on May 29, 2013.